Smart hip Implant Design

Finite Element Analysis

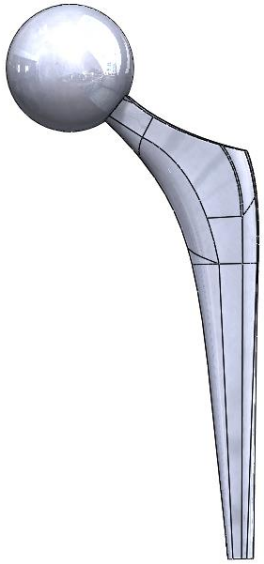

Xinyue(Alina) Zhang

02217044

Table of Contents

1. Introduction

A hip implant is a medical device used to replace damaged or diseased parts of the hip joint. This report uses FEA (Finite Element Analysis) to ensure safety and predict potential points of failure and the overall longevity of the implant.

The initial design is simulated with static and alternating loading situations to determine the fatigue conditions and whether the implant can sustain structural integrity for 15 years. In addition, a frequency analysis is conducted to ensure that the natural frequency of the implant falls in the range of 100 to 3000Hz for vibration-based NDT (non-destructive testing) to monitor the health of the implant.

A further revised design is proposed and tested, with the titanium version satisfying the requirements.

2. Methodology

2.1 CAD model

The CAD model is obtained from an online open resource[1] with the insert and cup removed from the original design. By taking the density of Ti-6Al-4V as 4.43g/cm^3[2], the total mass of the implant without the insert and cup is 178.5g. The mass of a lightweight hip implant without the cup and insert is approximately 173g-217g.[3] The design falls in the range, thereby satisfying the requirement of 'Lightweight'. The model is carried further for FEA tests to examine its feasibility and tolerance in real-world applications.

Figure 1 : CAD model of the hip implant without the Acetabular Cup and Polyethylene Insert

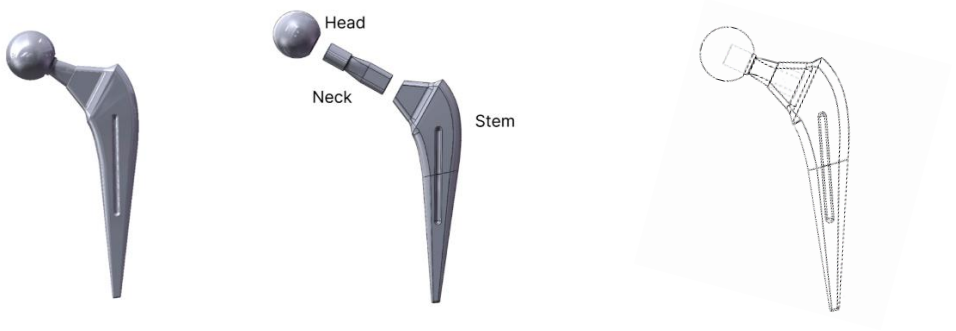

Table 1: Dimensions and data of the hip implant

Overall Length	166.35 mm
Volume	40293.88 mm^3
Surface Area	10777.36 mm^2
Stem	
Stem length	141.9 mm
Stem width	44.11 mm
Stem thickness	11.96 mm
Neck	
Neck length	43.96mm
Neck width	14.00 mm
Neck Thickness	12.00 mm
Head	
Head Diameter	30mm

2.2 Assumptions

1. The analysis excludes the acetabular cup and polyethylene insert.
2. The head, neck, and femoral stem are combined as a single component
3. The hip implant is made of Titanium alloy(Ti-6A-4V) or Stainless Steel 316L.
4. The hip implant is embedded in the femur and subjected to a vertical force along the axis of the body which oscillates between zero and 2490N without safety factor.
5. The deposition and displacement of during daily activities is ignored.
6. Gravity in the environment is ignored.

2.3 Boundary Conditions

2.3.1 Fixed Support

The implant is 'fixed supported' from its tail to halfway through its length. Both the translational and rotational degrees of freedom (D.o.F) in all directions are set to zero. This fixation is achieved either by cement filling or by the bone surface directly (Fig.2). [4]

Figure 3: Fixed support on model

Figure 2 : fixed support in femur [4]

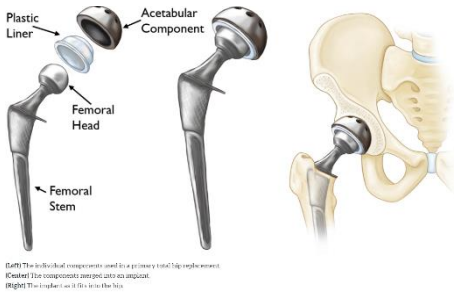

2.3.2 Loads

The static simulation load is a constant 2490N, while the fatigue analysis load oscillates between 0 and 2490N. These values are realistic estimations based on typical daily activities, but the number can differ greatly by different body weights (Fig.4).

Figure 4: **a.** Loading of different activities [5] **b.** loading on cartesian axis [6] Figure 5: Force applied

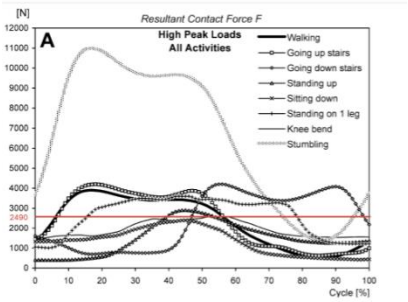

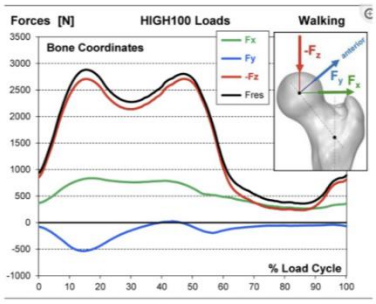

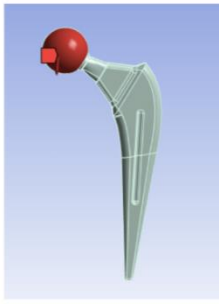

The force is applied on to the head by the pressure from the acetabular cup and insert implanted in the hip. Although the ISA suggested a 9-10° loading along the axis of the stem, recent research suggests that the load is mostly exerted on the Z axis (on the vertical axis of the body). [6] This supports the rationale of applying the load vertically.

2.4 Material S-N curves

2.4.1 Ti-6Al-4V

Figure 6 : S-N curve of Ti-6Al-4V Left:[7] Right:[8]

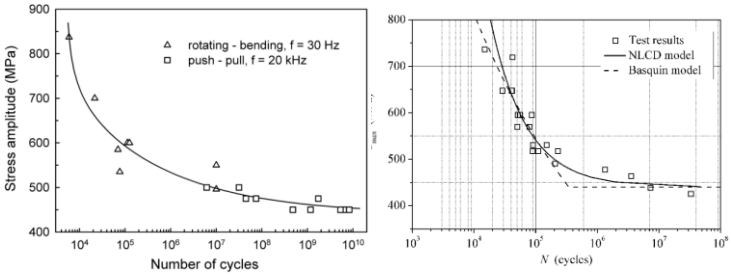

Figure 7: Digitized data plot

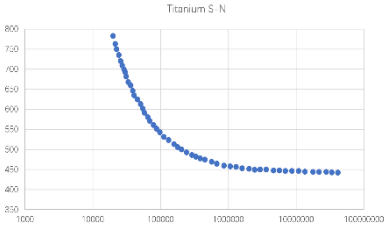

The S-N curve of Ti-6Al-4V is obtained by digitizing available research results (Fig.6). The two curves by different researchers have high similarities and are combined to generate comprehensive results. The resulting digitized data is plotted against the original plot to confirm the accuracy.

2.4.2 Stainless Steel 316L

Figure 8: The S-N curve of stainless steel

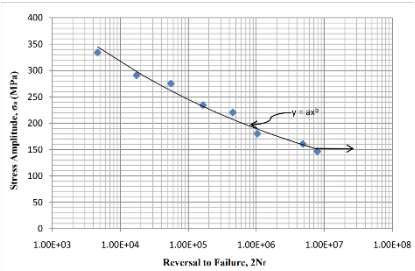

Figure 9: Plotted S-N curve after digitization

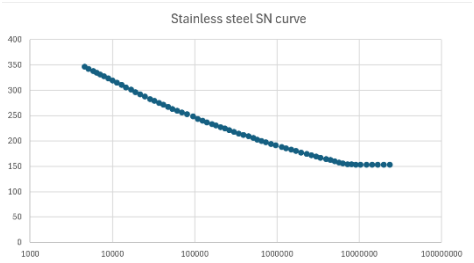

The S-N curve of stainless steel is obtained using the same approach. However, disagreements between the data are noticed due to different environments and types of stainless steel 316L used (life, initiated, treated, untreated). Given the unspecified type of stainless steel 316L in the brief, the S-N curve of austenitic type 316L stainless steel is selected for its prevalent use in medical equipment.[9]

2.5 Static Simulations Parameters

Before proceeding to fatigue simulations, the static analysis is conducted to ensure that the current design withstands the maximum load of 2490N vertically downward along the axis of the body. Both Titanium and stainless steel are ductile, therefore Von-Mises Criterion is employed, which defines that at a point within the domain, the material fails if:

$$\sigma_v > S_y$$

The Tresca criterion could also be applied, however, this design emphasizes 'lightweight', which aims for reduced material. Therefore, it is not considered.

2.6 Fatigue Simulations Parameters

In daily movements, the hip joints are subjected to changing cyclic loads which can cause mechanical failures well below the yield or ultimate strength. Microscopic cracks often appear at stress raisers and then continue to grow with fluctuating loads, resulting in fatigue.

The load is applied as a coordinated sine wave oscillating from 0 to 2490N (Fig.11). The stress result is then compared to the material SN curves to determine its ability to withstand 15 years of lifetime (five million loading cycles).

The estimation of 5 million loading cycles suggested by ISA is rather conservative and a normalized value of 10 million cycles is more realistic, especially for titanium hip implants [5].

Figure 10: Loading cycles [5]

Load cycles and cycle times

Activity	Cycle time T (s)	Normal patients cycles (1000)		Active patients cycles (1000)	
		Per year	Normalized	Per year	Normalized
Walking	*1.10*	*1369.3*	*10,000*	*2553.4*	*10,000*
Going up stairs	*1.59*	*41.4*	*300*	*140.2*	*550*
Going down stairs	1.44	41.4	300	140.2	550
Standing up	2.49	20.1	150	64.6	250
Sitting down	3.72	20.1	150	64.6	250
Standing on 1 leg	6.70	63.5	460	126.6	500
Knee bend	4.67	–	–	–	–
Stumbling	*1.10*	*0.120*	*0.90*	*0.120*	*0.55*

Notes: Values for 'normal patients' and 'active patients'. The cycle numbers per year for walking were increased to 10 million ('normalized') for both patient groups, and the numbers for the other activities were increased proportionally and rounded up. The activities printed in italic constitute the test scenario for 'high-impact activities'.

Figure 11: Cyclic loading

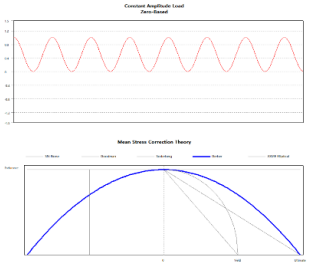

The stress ratio is zero (R =σmin/σmax = 0/2490 = 0). Due to the ductile properties of the materials, Gerber correction is applied to correct the value for the alternating stress. The stress is obtained from the maximum von Mises stress from the simulation with the maximum static load.

$$S_{ca} = \frac{S}{1 - (\sigma_{mean}/S_u)^2}$$

2.7 Frequency Simulation Parameters

The frequency of the oscillating load is less than 40 cycles per hour (5 million for 15 years), equivalent to 0.01 Hz. This indicates that the loads vary extremely slowly making the inertial effects negligible and the frequency simulation quasistatic. Therefore, the equilibrium equation of the FE model is:

$$[\boldsymbol{K}]\{\boldsymbol{D}\} = \{\boldsymbol{R}\}$$

The vibration of the system is assumed to be undamped. The damping effect is removed due to its marginal effect. Five natural frequencies are compared with the frequency range of 100 Hz-3000 Hz to design an effective vibration-based test for monitoring the health of the implants.

3. Results

3.1 Mesh Refinement

3.1.1 Initial meshing and sanity check

An initial mesh is sized at 10mm and set to linear to find the stress concentration points and perform a **sanity check** of the usability of the model.

Figure 12: 10mm meshing and areas of stress concentration.

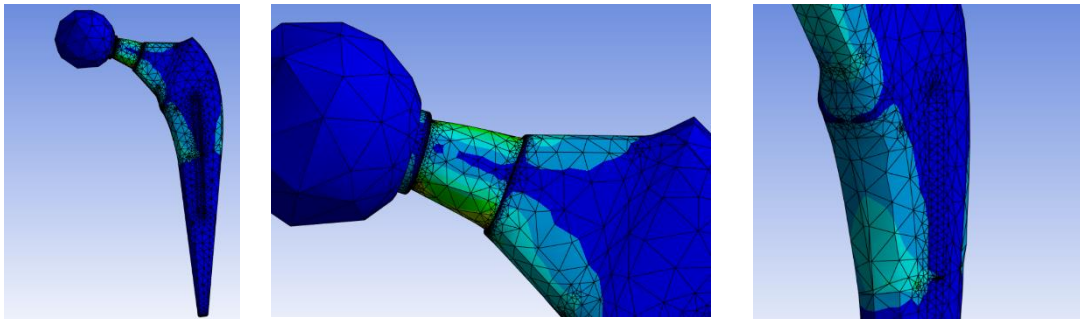

As shown in Fig.12 the stress is mostly concentrated along the upper and lower sides of the stem and neck. The aspect ratio of most of the meshes is 4.84, with a maximum of up to 74.432 in the same position as the stress concentration area. This is higher than the desired range of 1 to 3 and therefore is not acceptable. In addition, the defeaturing of some boundaries has changed the geometry of the implant which could deflect the result. Therefore, global mesh refinement is conducted.

3.1.2 Global h-refinement

The correlation between the maximum equivalent (von Mises) Stress and the element size is investigated by iteratively decreasing the mesh size by 2mm. The defeaturing warning disappears at 6mm, and the stress converges from 4mm to 1mm. A safer and more conservative 2mm is selected.

Figure 13: Maximum equivalent stress vs element size

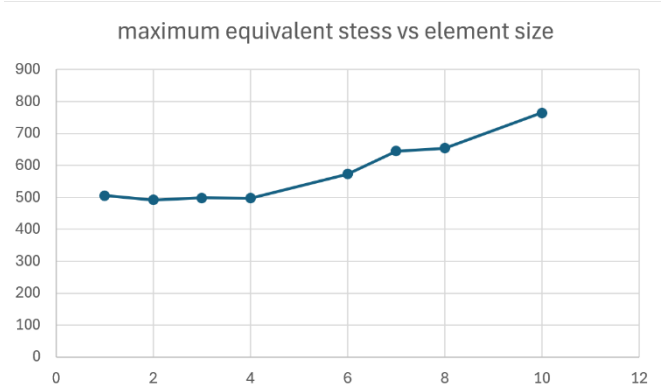

The aspect ratio already satisfies the requirements with over 4.6 x 10^4 meshes with a ratio of 1.16, and only 804 meshes beyond the range. The areas of high aspect ratio are identified

as shown in Fig.15. This occurs at sharp edges of connection between parts.

Figure 14: aspect ratio graph

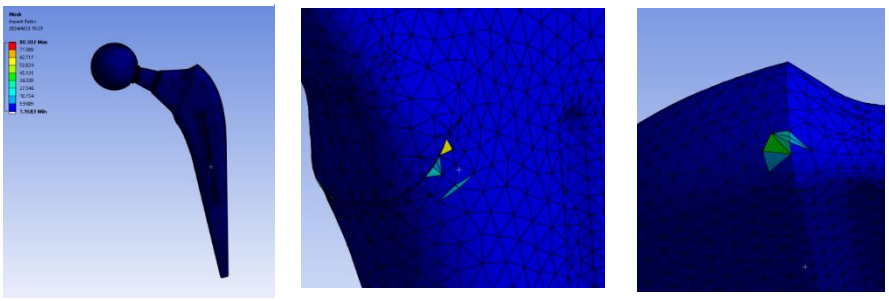

3.1.2 Global p-refinement

The head and the stem consist of smooth curves, which might require a quadratic interpolation method to add nodes on the existing mesh boundaries to simulate.

Figure 15: Equivalent stress and element size correlation

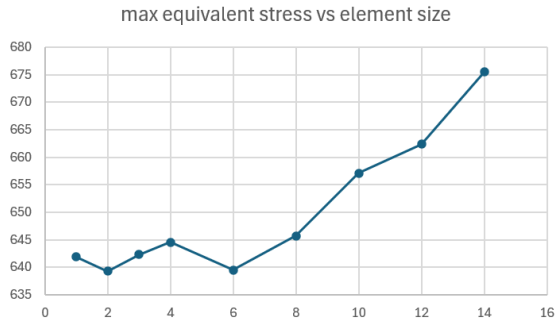

However, the stress does not converge with reductions in mesh size which creates difficulties when selecting the mesh element size.

Figure 16: Mesh quality plot of linear(upper) mesh and quadratic (lower) mesh

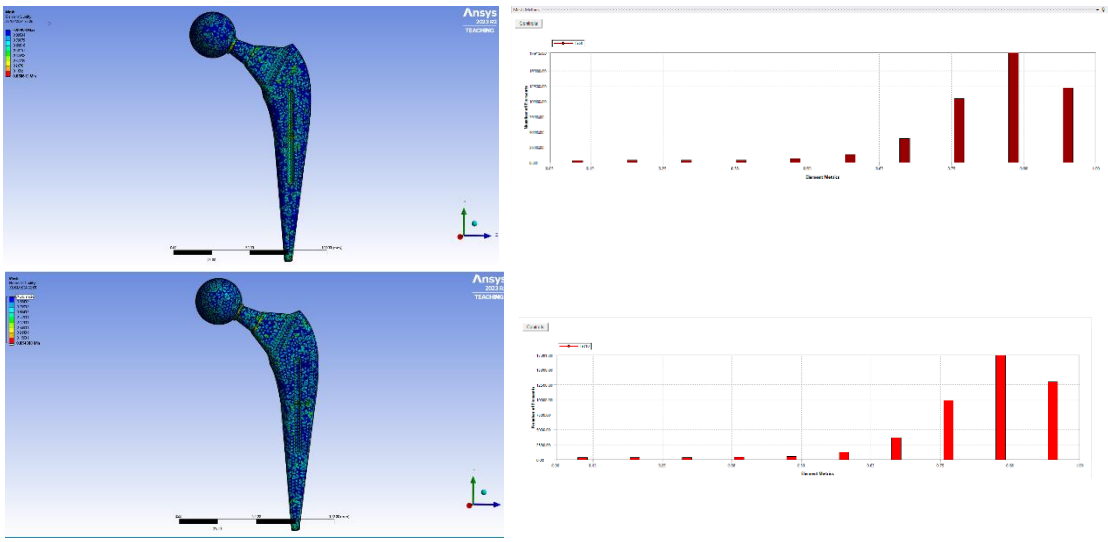

In addition, when comparing with the linear mesh of the same size, the element quality has very marginal improvements with only the mesh quality already exceeding the minimum requirement of 0.8, slightly improved. To reduce the computational time and save hardware ability to process data, the linear element is used. In areas with low mesh quality, local mesh

refinement is conducted.

3.1.2 Local refinement

Figure 17: **a.** element quality graph (left), **b.** stress concentration (middle), **c.** local meshing (right)

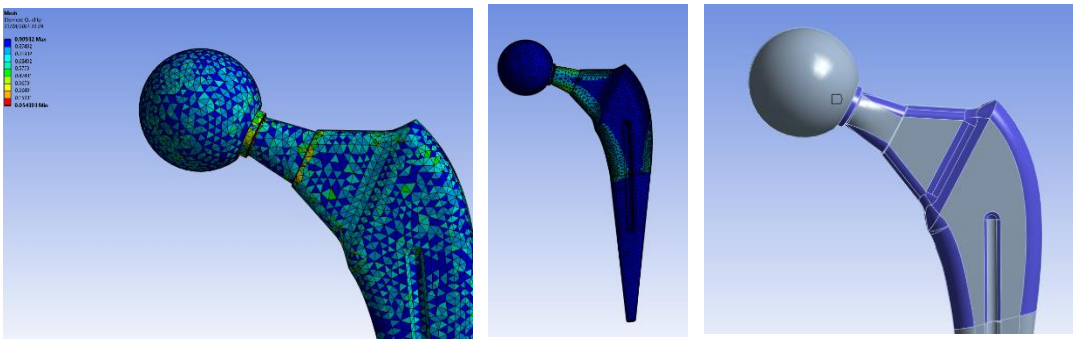

As shown in Fig.17.a, the mesh quality at the welding connection between the head and the neck is evidently lower, where the aspect ratio is also beyond 3. In addition, stress concentrates along the sides of the neck and the stem (Fig.17.b). To reduce the discretization error and improve the accuracy of the model, local refinement is conducted in these areas (Fig.17.c). The local mesh size is reduced from 3mm to 0.5mm iteratively. The stress stabilizes in the range of 1mm to 3mm and diverges from 0.5mm where it reaches the hardware limitation.

Figure 18: The max equivalent stress vs local mesh element size

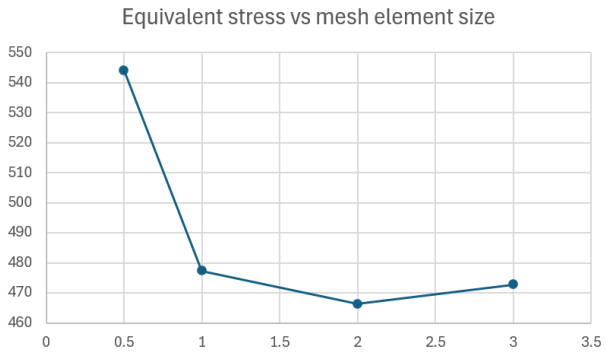

1mm local mesh size is selected for its ability to eliminate meshes of aspect ratio above 3 both on the surface and internally (Fig.19). The **sanity check** suggests Jacobian ratio remains at 1, and the aspect ratio is 1.16 for 5.9 x 10^4 meshes, with only 0.2% of outliers. Also, the refinement causes a decrease of the stress from 505.7MPa to 477.3MPa by 7%.

Figure 19: Aspect ratio graph before(left) and After(right)

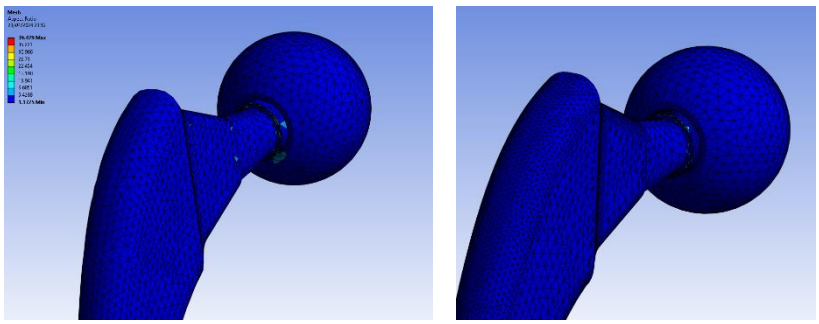

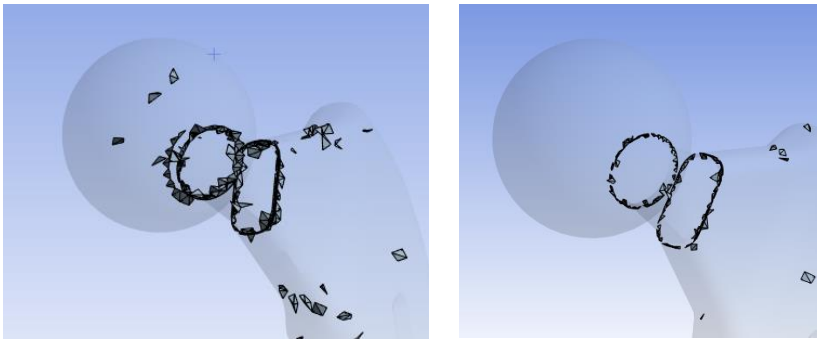

3.2 Fatigue analysis

3.2.1 Static analysis result

Figure 20: von Mises strength concentration of a. Ti-6Al-4V(left) and Stainless steel 316L (right)

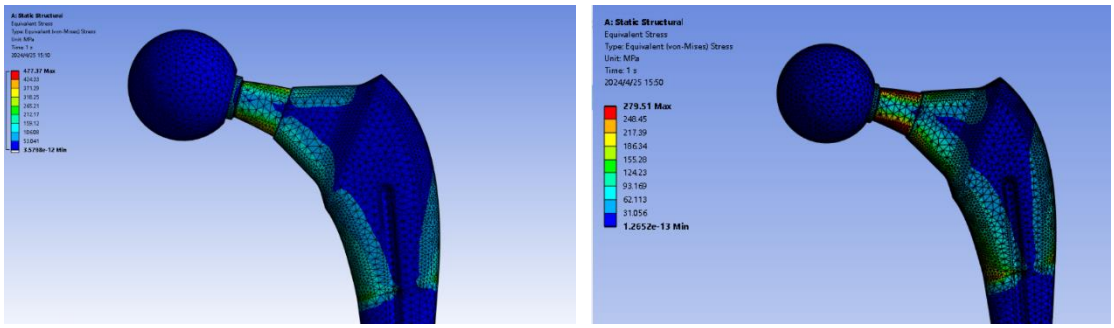

Based on the von Mises criterion, the material fails if the von Mises stress is greater than the yield strength when the material starts to plastically deform.

$$\sigma_v > S_y$$

The yield strength of the Ti-6Al-4V is 845.73 MPa, which is larger than the maximum von Mises strength (477.37 MPa). This indicates that the structure does not fail with static loading.

However, the maximum von Mises stress of Stainless steel is 279.51MPa, greater than the yield strength of 228MPa. Therefore, stainless steel cannot sustain the static load with current design. The failed element is nucleated around the neck area, which provides opportunities for further iteration.

3.2.2 Fatigue analysis result

The fatigue result is generated with zero-based loading and Gerber correction. The corrected stress result is then compared with the S-N curve to identify the corresponding number of cycles. According to the result generated, all parts of the implant have infinite life. A possible explanation is that the stress exerted on the implant is small enough that cyclic loading is unable to produce microscopic failures or cause fatigue on the model.

Figure 21: Fatigue result of titanium and stainless steel

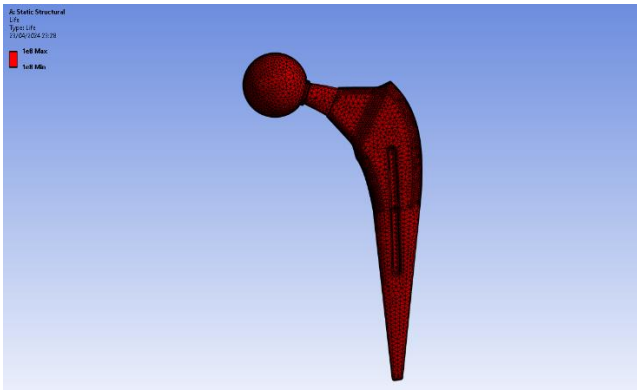

To verify the result, a **sanity check** is conducted with $\sigma_{min} = 1.158 \text{ x } 10^{-11} MPa$ and $\sigma_{max} = 477.37 MPa$ .The means stress and alternating stress are:

$$\sigma_{mean} = \frac{\sigma_{max} + \sigma_{min}}{2} = \frac{1.158 \text{ x } 10^{-11} + 477.37}{2} \approx 238.69 \, MPa$$

$$S = \frac{\sigma_{max} - \sigma_{min}}{2} = \frac{477.37 - 1.158 \text{ x } 10^{-11}}{2} \approx 238.69 \, MPa$$

The corrected alternative strength is:

$$S_{ca} = \frac{S}{1 - (\sigma_{mean}/S_u)^2} = \frac{238.69}{1 - (238.69/911.826)^2} = 256.23 MPa$$

The corrected alternative stress is below the S-N curve of Ti-6Al-4V (Fig.6) with a minimum of 307MPa. This shows that the alternating stress does not affect the life of the model. The number of cycles is therefore reasonable and beyond the requirement of 5 million cycles.

Although the fatigue result of stainless steel is less important due to its failure in static loading conditions, the result is valuable for iteration. The results given by the software analysis also show an infinite life cycle. By a similar approach, the corrected alternating stress is 149.34 MPa, which is also below the S-N curve minimum of 245MPa.

3.3 Frequency analysis

Figure 22: frequency analysis result **a**. Titanium (upper) **b.** Stainless steel (lower)

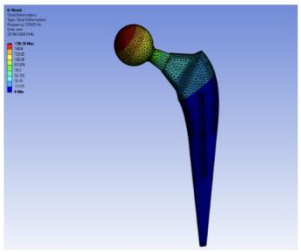

Tabular Data

	Mode	Frequency [Hz]
1	1.	579.03
2	2.	1199.9
3	3.	2270.7
4	4.	3148.6
5	5.	3779.3
6	6.	6402.2

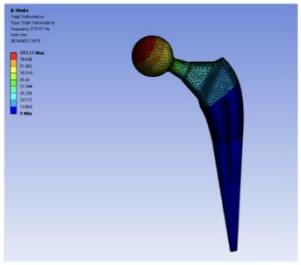

Tabular Data

	Mode	Frequency [Hz]
1	1.	575.47
2	2.	1183.
3	3.	2242.1
4	4.	3166.5
5	5.	3724.3
6	6.	6369.7

The first, second, and third order frequencies are within the range of 100Hz–3000Hz, however, the fourth and fifth orders are beyond 3000 Hz. This reflects the opportunity of re-designing to have better detectability to be monitored.

Sanity check:

Because of the undamped free vibration assumption, the natural frequency of the implant is related to the stiffness and mass of the material.

$$\omega = \sqrt{\frac{k}{m}} \text{ and } \omega_n \propto \sqrt{\frac{E}{\rho}}$$

The same geometric is used for titanium and stainless steel, Therefore, the natural frequency difference between the two materials depends on the ratio of Young's modulus over density.

Table 2: natural frequency comparison between two materials

	Titanium	Stainless steel
Young's modulus	113.9 GPa	195.122 GPa
Density	4428.73 kg/m^3	7969.37 kg/m^3
(E/ρ)^1/2	0.16	0.156
Natural frequency (1st order)	579.03 Hz	575.47Hz

The results show that there is little difference between the ratio of stiffness over density, and therefore the natural frequencies are nearly identical.

3.4 Design Revision

Several design considerations are proposed to improve the model.

1. The sharp edges and cavities near the welding connections should be reduced for better quality meshes and less concentration of stress.
2. The stainless-steel implant fails around the neck area during static loading, and the stress needs to be distributed.
3. The natural frequencies fall out of the range of 100Hz-3000Hz, and the fourth and fifth natural frequencies should be decreased.

Figure 23: Iterations of the model

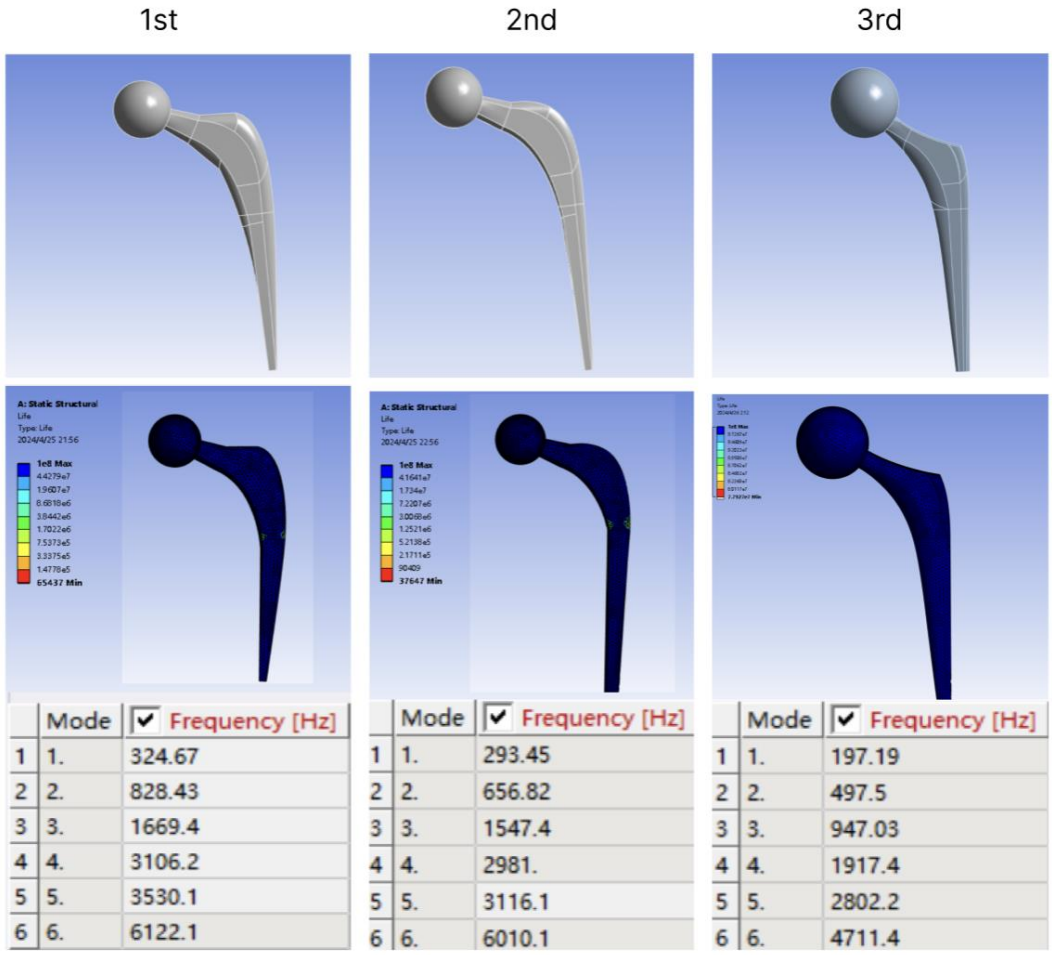

	Mode	Frequency [Hz]
1	1.	324.67
2	2.	828.43
3	3.	1669.4
4	4.	3106.2
5	5.	3530.1
6	6.	6122.1

	Mode	Frequency [Hz]
1	1.	293.45
2	2.	656.82
3	3.	1547.4
4	4.	2981.
5	5.	3116.1
6	6.	6010.1

	Mode	Frequency [Hz]
1	1.	197.19
2	2.	497.5
3	3.	947.03
4	4.	1917.4
5	5.	2802.2
6	6.	4711.4

The first model smooths the surface for better mesh refinement. Global mesh is set at 2mm, and local mesh of 1mm is applied along the stress concentration area as proceeded from the mesh refinement from the initial model. A **sanity check** confirms the result with an aspect ratio of 1.16 for 99.7% meshes, and a Jacobian ratio equal to 1.

The second iteration aims to reduce the natural frequency which can be calculated as follows:

$$\omega_n = {a_n}^2 \sqrt{\frac{E\,I}{L^3 m}} = {a_n}^2 \sqrt{\frac{E\,I}{\rho\,L^4 A}}$$

In the equation, a_n is a constant of the order of the frequency, and E is the Young's

modulus of the material used. To reduce the natural frequency, the mass m and the length of the model L should be increased, and the second moment of area I should be decreased.

Figure 24: **a.** cross-section of the implant **b.** eclipse moment of area [10]

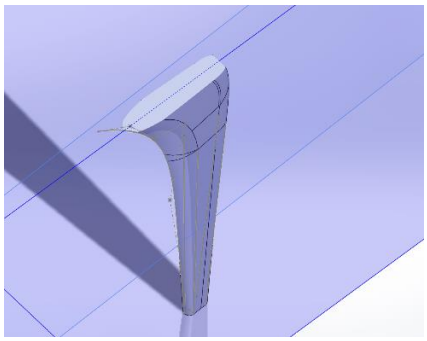

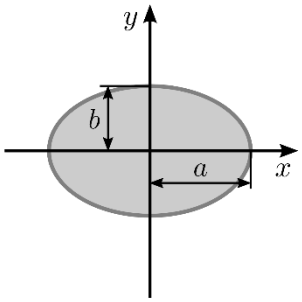

$$I_x = \frac{\pi}{4}ab^3$$

$$I_y = \frac{\pi}{4}ba^3$$

$$A = \pi ab$$

$$\frac{I_x + I_y}{A} = \frac{1}{4}(a^2 + b^2)$$

The cross-section of the model is simplified to an eclipse. According to the deformation, the implant bends in both the x and y direction (Fig.24), therefore, for a lower $\frac{I}{A}$, both a and b (the width and thickness of the stem) are reduced.

The 4th natural frequency successfully falls in the range, but the stem is too thin to withstand the alternating stress, so the life decreases to only 30,000. To maintain the strength of the structure, the inclination angle of the neck is increased to decrease the moment by the vertical force and to distribute the stress from the neck area to the stem.

Figure 25: Final design

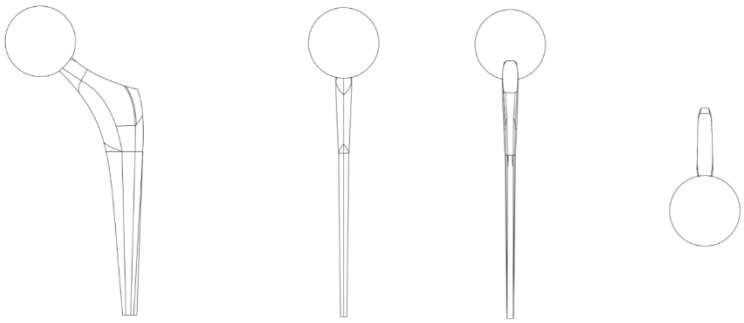

Table 3: Final design dimensions

Overall Length	187.33mm
Volume	48704.09mm^3
Surface Area	12898 mm^2
Stem	
Stem length	150.25 mm
Stem width	31.45mm
Stem thickness	9.2mm
Neck	
Neck length	23.38mm
Neck width	14.57 mm
Neck Thickness	9.43mm
Head	

Head Diameter	40mm

1.5 Revised Results

1.5.1 Static results

Figure 26: Static analysis of revised design

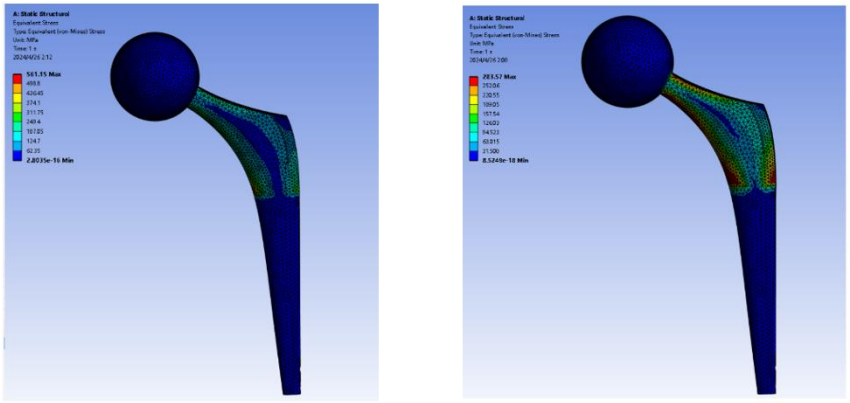

The maximum von Mises stress under static loading of Titanium is 561.15MPa, below the yield strength (845.73 MPa). According to the von Mises criterion, the titanium final design passes the test ($\sigma_v < S_y$) However, the stainless-steel version fails during the static loading test with the maximum equivalent stress of 283.57 MPa >228MPa.

1.5.2 Fatigue results

Figure 27: Fatigue analysis of revised design

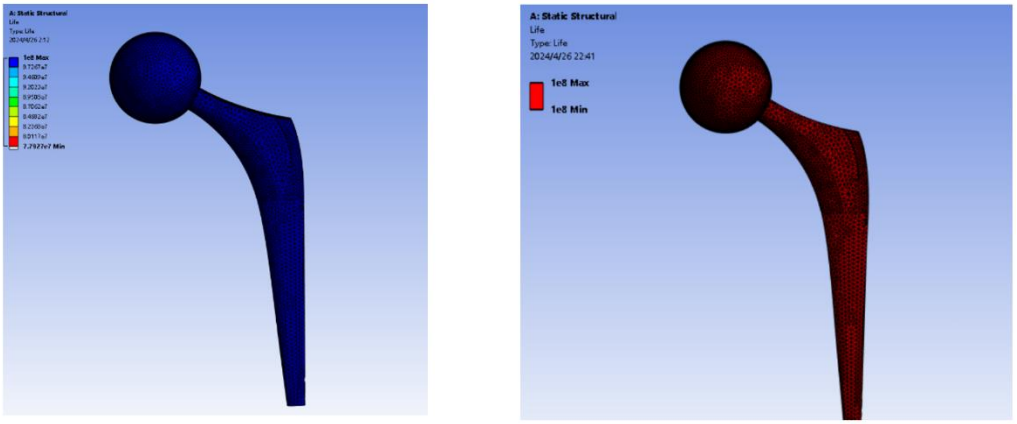

The life of the titanium implant is 7.8 x 10^7, which, although less than before, still satisfies the requirement of 5 million cycles. The stainless-steel implant still has 1 x 10^8 cycles of life. The **sanity check** approves the result, with the $\sigma_a = 309MPa$, slightly greater than 307MPa at 1 x 10^8 cycles for titanium.

1.5.3 Frequency result

Figure 28: Frequency analysis of the revised design of titanium (left) and stainless steel (right)

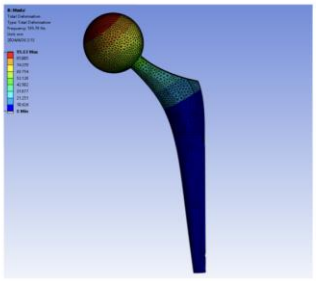

Tabular Data

	Mode	Frequency [Hz]
1	1.	195.79
2	2.	504.56
3	3.	942.33
4	4.	1944.3
5	5.	2846.6
6	6.	4788.

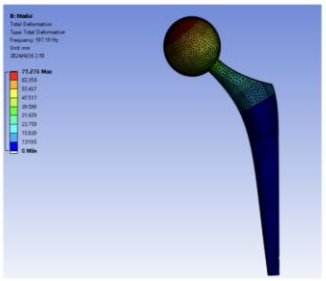

Tabular Data

	Mode	Frequency [Hz]
1	1.	197.19
2	2.	497.5
3	3.	947.03
4	4.	1917.4
5	5.	2802.2
6	6.	4711.4

Both the titanium and stainless-steel revised design have five natural frequencies within the range of 100Hz and 3000Hz. The fourth and fifth natural frequencies decreased by 38% and 24% respectively. The deformation also decreased by 40% which contributed to the stability of the implant. The natural frequencies of the two materials are similar as suggested in the initial sanity check.

4. Discussion and conclusions

Table 4: Summarized result of the hip implant analysis

Model	Material	Max von-Mises stress (MPa)	Fatigue life/ cycles	Natural frequency (Hz)	Mass (g)
Initial design	Titanium	477.37	1x10^8	579-3779	178.5
	Stainless steel	279.51	1x10^8	575-3724	322.4
Final design	Titanium	561.15	7.7x10^7	195-2846	215
	Stainless steel	283.57	1x10^8	197-2802	389
Requirement			5 x 10^6	100-3000	<300g

The revised titanium implant meets all requirements, but the stainless-steel implant deforms plastically under static loading. Overall, the titanium implant performs better than stainless steel with enhanced structural integrity and lighter weight.

Modelling Error:

1. The contact between the stem head and the cup is flexible which affects the direction of the force applied to deflect from the vertical axis.
2. The force exerted on the implant can defer greatly by the pelvis angle, weight, age, and pattern of movements of the patient.
3. The implant within the body is surrounded by muscles and tissue, causing additional stress and contact on the implant.
4. The deviances of S-N curves of different types of stainless steel 316L can cause inaccurate predictions of the life in fatigue analysis.

Systematic Error:

1. Discretization error can result in inaccuracy of the analysis. For example, there are small amount of mesh(0.2%) still beyond the aspect ratio requirement after the refinement.
2. Hardware limitations constrain the mesh refinements lower than 0.5mm, which reduces the accuracy of analysis.

In conclusion, although the model does not accurately simulate the real-world situation, it still suggests valuable insights to integrate implant design before carrying on to prototyping.

Word Count: 2649 (excluding bibliography, captions, and footnotes)

Bibliography

[1] S. McConnell, “Free CAD Designs, Files & 3D Models | The GrabCAD Community Library,” *grabcad.com*, Feb. 08, 2016. https://grabcad.com/library/prosthetic-hip-implant-1/details?folder_id=1653248 (accessed Apr. 17, 2024).
[2] A. Khorasani, I. Gibson, U. S. Awan, and A. Ghaderi, “The effect of SLM process parameters on density, hardness, tensile strength and surface quality of Ti-6Al-4V,” *Additive Manufacturing*, vol. 25, pp. 176–186, Jan. 2019, doi: https://doi.org/10.1016/j.addma.2018.09.002.
[3] S. Marmor *et al.*, “Doctor, what does my ceramic-on-ceramic hip arthroplasty weigh?,” *Orthopaedics & traumatology: surgery & research*, vol. 109, no. 1, pp. 103298–103298, Feb. 2023, doi: https://doi.org/10.1016/j.otsr.2022.103298.
[4] M. B. Cross, “Revision Total Hip Replacement - OrthoInfo - AAOS,” *www.orthoinfo.org*, Apr. 2017. https://orthoinfo.aaos.org/en/treatment/revision-total-hip-replacement/
[5] G. Bergmann, A. Bender, J. Dymke, G. Duda, and P. Damm, “Standardized Loads Acting in Hip Implants,” *PLOS ONE*, vol. 11, no. 5, p. e0155612, May 2016, doi: https://doi.org/10.1371/journal.pone.0155612.
[6] G. Bergmann *et al.*, “Realistic loads for testing hip implants,” *Bio-Medical Materials and Engineering*, vol. 20, no. 2, pp. 65–75, 2010, doi: https://doi.org/10.3233/bme-2010-0616.
[7] M. Janeček *et al.*, “The Very High Cycle Fatigue Behaviour of Ti-6Al-4V Alloy,” *Acta Physica Polonica A*, vol. 128, no. 4, pp. 497–503, Oct. 2015, doi: https://doi.org/10.12693/aphyspola.128.497.
[8] J. Lin, W. Li, S. Yang, and J. Zhang, “Vibration Fatigue Damage Accumulation of Ti–6Al–4V under Constant and Sequenced Variable Loading Conditions,” *Metals*, vol. 8, no. 5, p. 296, Apr. 2018, doi: https://doi.org/10.3390/met8050296.
[9] K. A. Mohammad, A. Ali, B. B. Sahari, and S. Abdullah, “Fatigue behavior of Austenitic Type 316L Stainless Steel,” *IOP Conference Series: Materials Science and Engineering*, vol. 36, p. 012012, Sep. 2012, doi: https://doi.org/10.1088/1757-899x/36/1/012012.
[10] Wikipedia Contributors, “List of second moments of area,” *Wikipedia*, Oct. 03, 2019. https://en.wikipedia.org/wiki/List_of_second_moments_of_area